MÉCANISMES DE FRAGILISATION PAR L'HYDROGÈNE DANS LES MÉTAUX: APPORT DES SIMULATIONS ATOMISTIQUES.

D. Tanguy[1], D. Connetable[2], Y. Wang[1,2], X. Schen[1]

[1] *Institut Lumière Matière, université de Lyon 1, Villeurbanne*
[2] *Cirimat Ensiacet, Toulouse*

dome.tanguy@univ-lyon1.fr
damien.connetable@ensiacet.fr

Mots clés : hydrogène, simulation Monte Carlo, rupture, dislocations.

1. INTRODUCTION

Le rôle de l'hydrogène dans la rupture des alliages métalliques "de structure" a été largement démontré expérimentalement. Néanmoins, il n'existe pas de modèle quantitatif, convaincant, à l'échelle microscopique. L'une des difficultés de l'étude de ce phénomène par simulation numérique est la diversité des échelles spatiales mises en jeu. Par exemple, dans le cas "semi-fragile", il est fréquent que la "process zone" s'étende sur plusieurs grains et soit le lieu de plusieurs types de rupture, comme le montre les faciès de rupture d'aciers, où coexistent des facettes de grains d'apparence fragile, du clivage (transgranulaire), des interfaces carbures/matrice fragiles et des ligaments ductiles. Ce genre de complexité est hors de portée de cet article qui se focalise sur la physique d'une pointe de fissure idéale, intergranulaire, à l'échelle nanométrique. Deux mécanismes sont généralement invoqués: la décohésion ou la plasticité intense et confinée (HELP: "hydrogen enhanced localized plasticity"). Cet article est la fusion de deux papiers de conférence récents qui paraîtrons dans "Proceedings of the International Hydrogen Conference 2012, Jackson Lake, Wyoming, Ed. B. Somerday and P. Sofornis". L'un porte sur l'étude des mécanismes de décohésion (une revue critique des calculs ab initio et une étude de l'influence de clusters de lacune sur la rupture), l'autre sur l'effet de H sur l'émission de dislocations, directement depuis la pointe (le rôle des sources extérieures n'est pas considéré).

2. ÉTUDE DES MÉCANISMES DE DÉCOHÉSION INTERGRANULAIRE: INFLUENCE DES AGRÉGATS DE LACUNES

Hydrogen can considerably modify the fracture behavior of normally ductile metallic alloys of face centered cubic structure by: (i) Enhancing the formation of intense and well localized slip bands that can lead to transgranular crack propagation (see [1] for a review of HELP); (ii) Triggering intergranular fracture. We consider that fracture is brittle when the crack runs along the core of the grain boundaries (like shown by post portem TEM for example in AlZnMg alloys [2]), but it does not require plasticity to be completely de-activated. In particular, in soft metals, like pure Ni [3], intergranular propagation is coupled to very intense plastic deformation in the matrix. One can imagine many different roles that plasticity can have in the damage of GBs: hardening of the matrix, enhance point defect production by dislocation-dislocation reactions, high local stresses at slip band-GB intersects, hydrogen localization... A useful concept, that can be used to make the modeling of this situation more tractable, is the local stress intensity factor k [4]. It supposes that a dislocation free zone of nanometric dimension exists just ahead of the crack tip. In this region, linear elasticity is valid (ahead of the brittle fracture process zone which is nonlinear). The plastic zone has a net shielding effect that is reflected by the gap between the applied stress intensity factor, far away from the plastic zone, K_a and k. Local k orders of magnitude are given by the Griffith criterion and are around 1MPa$\sqrt{m}$, while K_a is one or two orders of magnitude higher (most of the energy dissipated in fcc structures is plastic). In this framework, we follow the work of Thomson [4-7] and consider that brittle propagation is not possible if the k value for dislocation emission from the crack tip itself (k_{Ie}, in mode I) is lower than k_{Ic}, the critical stress intensity factor crack extension along the grain boundary. In the present work, atomistic simulations are used to understand how H modifies k_{Ie} and k_{Ic} by revealing the physical mechanisms involved in the crossover from intrinsic ductility ($k_{Ie}<k_{Ic}$) to brittleness ($k_{Ic}<k_{Ie}$). The link between k_{Ic} and K_{th} (the macroscopic threshold for crack propagation in the presence of H) is a complex multiscale problem [8], also involving H, that is not our purpose. In the following, we call decohesion the drop of k_{Ic} due to H.

A critical review of decohesion mechanisms can be found in [1]. One of the major questions is the local hydrogen concentration in the vicinity of the crack tip that is necessary for decohesion. Elastic calculations, in agreement with atomistics, predict a weak enhancement, of the order of a factor 2. The upper limits of bulk H concentrations commonly encountered experimentally are low (2000 at. ppm in Ni, 200 at. ppm in Al) which gives local concentrations below 1%. Ab initio calculations [9] have shown that surface formation energies, in single crystals, can be reduced almost to zero but it requires interplanar concentrations of the order of the monolayer i.e. at least 2 orders of magnitude higher than elasticity predictions. Recently, an ab initio based thermodynamic treatment of fracture [10] has shown that a constant H chemical potential and an imposed stress (the fixed extensive variable being the total number of metal particles) can induce a phase transition with an abrupt increase of interplanar H concentration and interplanar spacing. Another way to

present the results is to say that the applied stress to maintain a constant interplanar opening severely drops when a critical H concentration is reached. This decohesion mechanism is appealing (and has been found to operate at a grain boundary too [11]) but should be controlled by the rate at which H reaches the fracture process zone. Diffusion controlled embrittlement is well established at high temperature [12] but less clear in the case of H which diffuses fast.

Another way to obtain high local concentrations is to consider the density of deep traps in the GB. These traps can be saturated, at low temperatures, with reasonable bulk concentrations. This argument is used in [13]. Nevertheless, the impact of this segregated H in the Griffith balance is much smaller than the one from H occupying regular lattice sites [14,15]. This is coherent with experiments where traction are done on pre-charged samples, at various strain rates and which show that embrittlement is only obtained at low rates, i.e. segregated H is not enough to induce decohesion.

In this work we explore another source of GB damage: vacancies and the effect of their clustering into nano voids. To reduce the complexity of the simulations [16], we do not explicitly introduce H in the simulation and consider only vacancies in a pure metal (Al). We see two ways these nano voids could form in the presence of H: (i) Vacancy-hydrogen complexes slowly diffuse and cluster along the GB (like He bubbles form under severe irradiation conditions), in this scenario they are present all along the GB before the crack appears; (ii) the voids form in a process zone a few nm long ahead of the crack tip, where the stress concentration is large, but at a time scale given by the metal-vacancy exchange rate, which is out of reach of Molecular Dynamics. The first section of the paper is devoted to the way the clusters are generated, on a model bicrystal: the symmetrical tilt boundary $\Sigma=33(554)[110]$, in Al. Then, a crack is introduced along the GB and the impact of the vacancy clusters on dislocation emission is studied. Finally, brittle crack propagation is studied.

2.1 Generating vacancy clusters

The formation of intergranular vacancy clusters is a challenge for atomic scale simulations. Classical Molecular Dynamics can simulate physical times that are too short in comparison to the typical time for a vacancy-particle exchange (barriers for Al are 0.7eV at zero stress). Accelerated Dynamics methods such as those developed by Voter, and Kinetic Monte Carlo with event tables built on the fly are limited. There is often a large number of basins separated by low barriers and these events do not directly contribute to the evolution of the system on a large time scale. These methods are designed to give a dynamics that is as close as possible to the real one. As a first approach, we can avoid this and use equilibrium Monte Carlo (MC). Vacancies are defined with respect to a fixed reference lattice [17, 18]. In the Canonical ensemble, microstates are sampled by proposing displacement to the particles (these relax the system and introduce vibrational entropy in the simulation) and exchanges either to randomly selected vacancy-particle pairs or to first neighbor pairs. The trial states are accepted or rejected according to the Metropolis rule. The method generates a chain of configurations that eventually reach equilibrium. There is a dynamics which corresponds to the acceptance rates of the Metropolis rule but that should not be mistaken for the true dynamics (the one MD would generate). All the different stages of the void formation given below are the product of this stochastic dynamics.

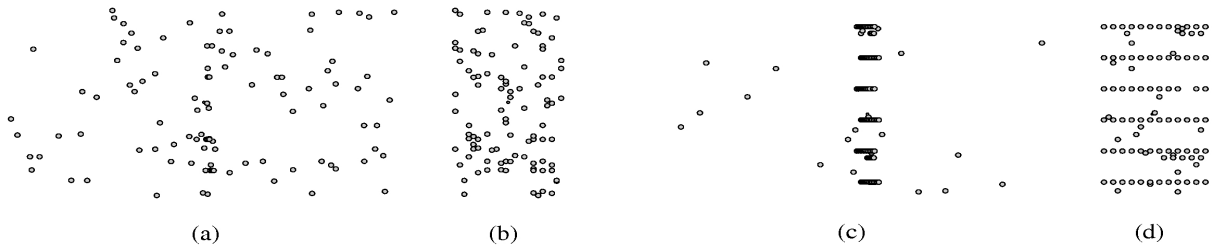

Figure 1: Vacancy ordering at zero stress and T=300K. (a) Initial distribution; (b) is a view from the side of (a). (c) At equilibrium vacancies are alined along the tilt axis (6 interfacial dislocations are contained in the box). (d) is a side view of (c).

We have found two cases. When the volume is adjusted to keep the stress close to zero, vacancies segregate to the boundary and aline along the tilt axis (Fig. 1). They induce large relaxations that can be viewed as an absorption to dislocation lines and subsequent climb. The results of the Monte Carlo simulation are confirmed by intensive free vacancy formation energy calculations on the sites of the GB, and vacancy-vacancy pair interactions. Following the scenario (ii) exposed in the introduction (where an intergranular crack creates a stress concentration that favors clustering ahead of the tip), the volume of the simulation box is stretched perpendicular to the interface. Then, vacancy trapping is largely reduced. If the initial configuration is the one obtained at zero stress (vacancy lines), vacancies that where initially dissolved re-localize and escape from the GB. If the initial concentration is large enough, vacancies cluster before they can reach the bulk. This out of equilibrium process gives a fine dispersion of intergranular vacancy clusters (Fig. 2a). Coarsening is obtained when exchanges between randomly selected particles and vacancies are performed (Fig. 2). Finally the simulation contains a single large cluster, with facets along {111}, in equilibrium with a low vacancy concentration in the bulk. Even if the sequence is the result of the stochastic dynamics, it was shown that the vacancy lines is the organization of the vacancies that minimizes the potential energy at low stresses, while clusters are more favorable above 4% stretch. The precise frontier between these two types of ordering, in the stress, concentration, temperature space, is a challenge for MC methods and will be the subject of a forthcoming paper.

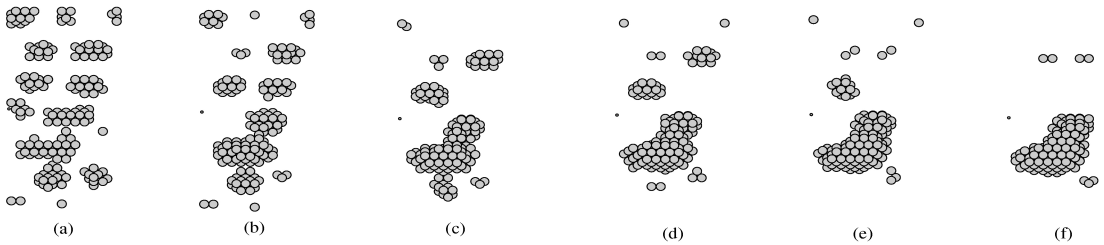

Figure 2: (a) Fine distribution of intergranular clusters obtained by MC simulation at 4% stretch perpendicular to the boundary, with first neighbor exchanges, starting from a configuration where the vacancies are alined along the tilt axis. (b) to (f): Coarsening.

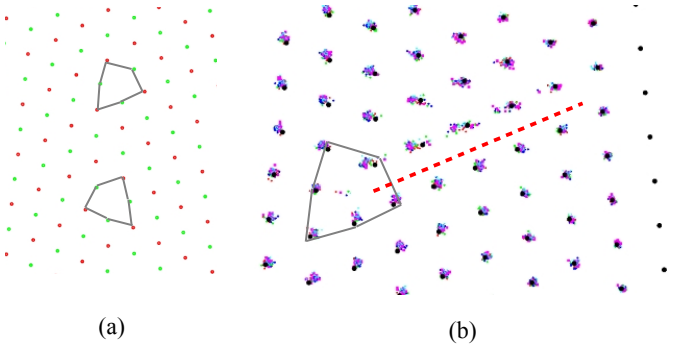

Figure 3: (a) Structure of the grain boundary. (b) Incipient dislocation emitted from a E structural unit. The black dots are the lattice positions, the colored dots are the projected positions of the particles at finite temperature.

2.2 Dislocation emission from the crack tip

The structure of the symmetrical tilt boundary Σ=33(554)[110] is composed of two structural units: E units underlined on figure 3 and twin boundary units (Σ=3). When a traction is applied perpendicular to the boundary, an incipient dislocation is emitted by each E unit. If we want to characterize the crossover from intrinsic ductility to brittleness, it is important to calculate k_{Ie} in the crack orientation where dislocation emission is the easiest, i.e. where the crack activates the emission from the E units. This is done when the crack propagation direction is y and the crack line lays along x (Fig. 1 and 3). With this orientation, there is one {111} plane that contains the crack line and is well oriented with respect to the z orientation along which the traction is applied in mode I. The orientation is such that an edge Shockley partial can be emitted with a line parallel to the crack line. The simulation box for the crack calculations is a thin parallelepiped approximately 3nm*100nm*100nm (800000 particles). A crack, approximately 6nm long, is introduced along the boundary, in the middle of the box, by removing atoms (Fig. 4a). Periodic boundary conditions are applied in the x and y directions, and the top and bottom layers in the z direction are fixed. Therefore, the crack is infinite in the x direction and weakly interacts elastically with its images in the y direction. The load, in mode I, is applied by imposing a constant displacement U_z to top fixed layers. For each value of U_z, the energy is minimized by Quenched Molecular Dynamics.

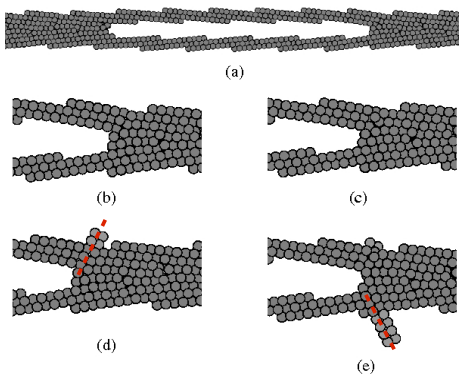

Figure 4: Dislocation emission for two different configurations of the clusters (the incipient Shockley partial is represented by light gray atoms above and below the glide plane). (b) Just before, (d) just after emission in the upper part of the box and (c), (e) in the lower part.

The left and right crack tips are not equivalent [19]. Dislocation emission occurs for much lower loads on the right, because the glide plane contains the crack line so an infinitely long dislocation line in the x direction can be emitted by shear localization at the tip. Five vacancy configurations are taken from the MC simulations. They are replicated along the crack plane and their influence on dislocation emission and on propagation is estimated. The results, concerning the critical load levels are shown on table 1. We see that the loads are low in comparison to the ones for propagation, whatever the vacancy configurations, but sometimes it is more difficult than others. There is a complex interplay between the structure of the grain boundary (the distance of the closest E unit to the crack tip), crack tip surface reconstruction and the void structure. It is illustrated on figure 4 where, depending on the vacancy configuration, the dislocation can be emitted in the upper part of the bicrystal or on the lower part.

Table 1: Table of the critical load levels obtained by traction simulations on systems containing vacancy clusters obtained from MC simulations under tension. "-" means: was not possible to evaluate due to massive dislocation emission and twinning.

Name (number of vacancies)	**Damage** (total void volume in number of dots)	Critical load for **propagation to the left** (U_z)	Critical load for **propagation to the right** (U_z)	Critical load for **dislocation emission** (U_z)
192 conf1	7536	-	-	3.0
241 conf1	9741	-	-	4.0
192 conf2	11307	5.0-5.5	-	3.0
241 conf2	14830	3.0-4.0	5.5	>4.0
271	16452	4.5-5.0	4.5-5.0	3.0-4.0

2.3 Fracture

Table 1 gives a list of configurations taken from MC simulations sorted by increasing "initial damage". This "damage" is characterized by the total void volume prior traction in preference to the total number of vacancies because these can dissolve in the GB. The three last configurations are shown on figure 5 to 7. Each colored stripe on these figures is a snapshot taken during energy minimization representing the voids viewed from the z direction (the direction of the applied traction) and the crack (center) during the fracture process. How this propagation is obtained is explained in the next paragraph. At the bottom of each figure is the initial configuration and, at the top, the final one. The pictures give an idea of the size and density of the clusters ahead of the crack, which is quantified by the void volume in Table 1. Even at high levels of initial void volume, dislocation emission always appears first, at loads between 3 and 4 (table 1). It seems that the crack is always intrinsically ductile. This is because the dislocations shield the load applied to the crack and close the opening ahead of the crack tip by their plastic displacement field. Therefore, crack propagation should not be possible, at least on the right side of the crack. We should comment on the possible brittle propagation from the left side, reported in [19]: First, dislocations emitted on the right induce a blunting and an elastic shielding that influence the effective load on the left side. There is no longer a simple relation between U_z and k. Second, the orientation of the easy glide planes is such that if the crack slightly deviates from the y direction, the symmetry is broken, and half loops are emitted. Therefore, it is important to test the impact of clusters on both crack tips because they are, in reality, both intrinsically ductile in the absence of initial damage.

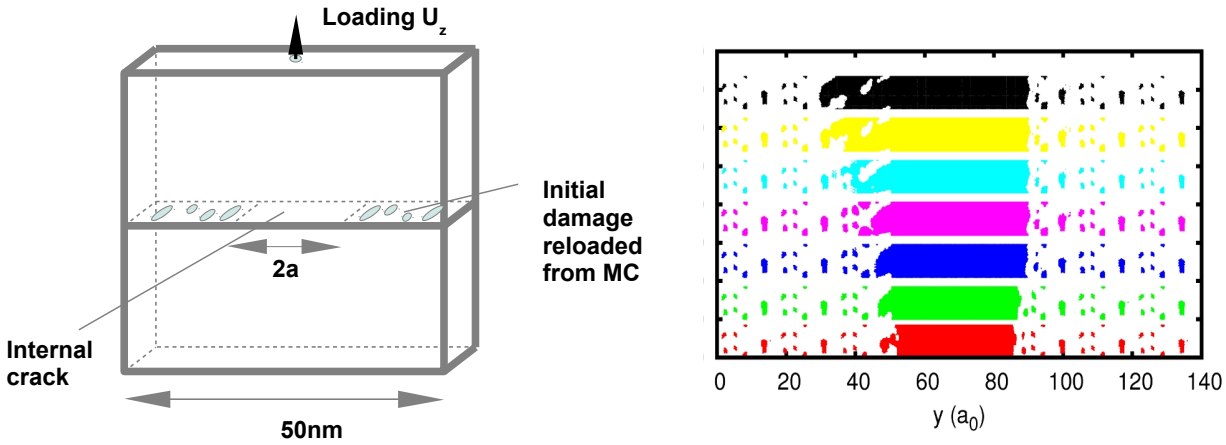

Figure 5: (left) A schematic drawing of the fracture set up. (right) Crack propagation obtained by constrained QMD at U_z=5.5 with cluster configuration "192 conf2" (table 1). Each stripe is a snapshot of the voids. Traction is in z, perpendicular to the picture. Increasing time is upward. The crack propagates only to the left.

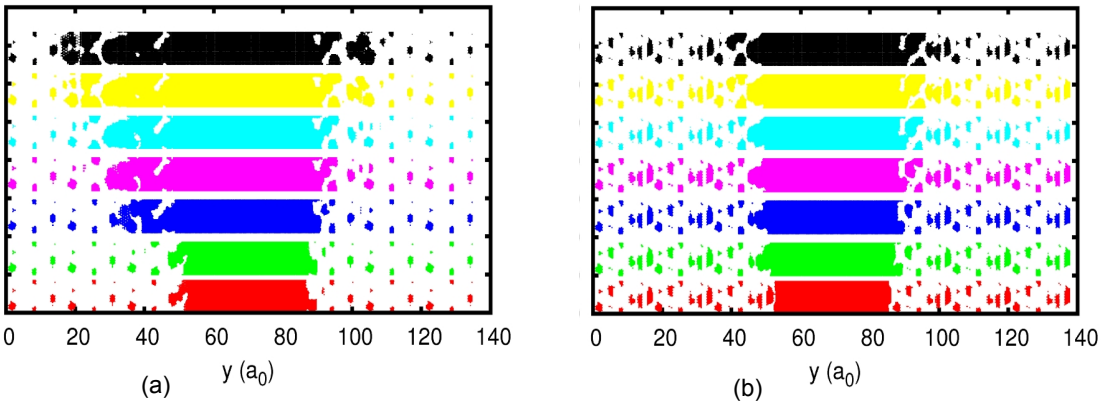

Figure 6: (a) Crack propagation obtained by constrained QMD at U_z=4.0 with cluster configuration "241 conf2" (table 1); (b) Crack propagation obtained by constrained QMD at U_z=5.0 with cluster configuration "271" (table 1). Initial damage increases from figure 5 to figure 6b (see table 1).

Ideally, we should determine k_{Ie} or k_{Ic} by incremental load raises, followed by an MD trajectory integrated up to macroscopic timescales. We replace this by the sequence: MC generation of different void configurations by the vacancy aggregation, under high tractions, characterization of the initial void volume and test of the stability of the crack by incremental load raises followed by Quenched MD. In the last step, we use a constraint in the equations of motions which prevents shear localization in the vicinity of the tip, still allowing crack propagation [20]. This gives access to the theoretical load for fracture. Even with the constraint, it was not possible to obtain any crack propagation for the two lowest damage levels ("-" in table 1). Increasing the damage level first triggers crack propagation on the left side. Figure 5 illustrate this and reveals a complex 3D void growth and coalescence with the crack tip. The crack is bridged. At higher damage levels (Fig. 6 and 7), crack propagates to the right, at higher loads.

2.4 Conclusion of the fracture study

By combining MC simulations and quenched MD, we studied the impact of realistic intergranular vacancy clusters on dislocation emission and theoretical brittle propagation. We found the cluster concentration that triggers unstable crack propagation but it occurs at load levels still high in comparison to those for dislocation emission. The implication is that a finer characterization of the effective load for dislocation emission, possibly including effect of segregations, is required together with fracture simulations at finite temperatures.

3. ÉTUDE DE L'INFLUENCE DE H SUR L'ÉMISSION DE DISLOCATIONS PAR UNE POINTE DE FISSURE

Hydrogen effects on plasticity have been intensively studied experimentally in the past. Observations at a fine scale, using environment cell TEM, have shown enhanced dislocation mobility and high localization of plasticity (for a review of HELP see [1]). The phenomena are emphasized at, or close to, crack tips where H concentration is larger than the average. They can have drastic effects on the mechanical strength of normally ductile metallic alloys by promoting transgranular fracture by intense and localized plastic shear. Some of these effects have been successfully modeled in the framework of elasticity [21,22], like the shielding of dislocation interactions, others like dislocation emission from a crack tip need to be investigated at the atomic scale. The Embedded Atom Method [23] is an efficient tool to study H defect interactions, in particular in Ni [24-26].

In the present work, we deal with systems and concentration-temperature conditions where hydrides are not stable. The focus is on H impact on fracture, in the framework of the Rice and Thomson model. These authors proposed [27] to separate brittle from ductile materials by quantifying the critical load for emitting a dislocation directly from the crack tip and comparing it to the ideal load for crack propagation, given by the Griffith criterion. Crack tip loading is best characterized by the stress intensity factor (SIF): k_I, in mode I; k_{II} in mode II. In terms of SIF, the Rice and Thomson criterion is $k_{Ie}>k_{Ic}$ for a brittle crack, where k_{Ie} is the critical SIF for emitting a dislocation from the crack tip, in mode I and k_{Ic} is the Griffith load given by $k_{Ic} = \sqrt{(E2\gamma_s)}$ where γ_s is the surface energy. In most metals, when the crack orientation is such that the tip intersects a slip plane, $k_{Ie}<k_{Ic}$: a crack spontaneously emits dislocations and is blunted. From experimental observations, it is clear that H should change this picture, in case of intergranular crack propagation. It should induce a decrease of k_{Ic}, but can also act in any direction for k_{Ie}. For example, k_{Ie} could increase in the case of the formation of a local hydride [25,26]. Most likely, as considered in HELP, H could enhance dislocation emission at the crack tip. The goal of the present work is to quantify the magnitude of the effect, by using simulations based on EAM potentials and DFT calculations.

The calculation of k_{Ie} by DFT relies on the analytic model developed by Rice [28]. In a similar way as k_{Ic} is related to the surface energy, it relates k_{Ie} to the unstable stacking fault energy γ_{us} [29]. In the original model, γ_{us} is the energy barrier produced by a rigid block shearing of the crystal in the glide direction. The model is exact only in mode II ($k_{IIe} = \sqrt{(2\gamma_{us}\ \mu/(1-\nu))}$). In mode I, k_{Ie} depends also on the formation energy of a step at the crack tip [30,31]. Thomson suggested that the model could be adapted to mixed mode (i.e. dominant mode II, and moderate mode I or III additional

load) if γ_{us} is modified to account for the relaxations induced by mode I [32] and mode III. Taking into account these constraints, we will use the Rice model for the emission of a dislocation, in mode II, along the crack plane, but with a superimposed mode I to induce H segregation ahead of the crack tip. We will show that EAM potentials, in pure Al, can be used to determine the relaxations, due to the mode I component of the load, to be included in the γ_{us} calculation. Preliminary DFT results are given in the pure metal case. In a second part, H is considered. The solute introduces new distortions at the crack tip. It is not clear at the moment how they should be included in the calculation of γ_{us} [33,34]. We present first results where H segregation to an ideal, sharp, crack tip is studied by an EAM potential. DFT calculations, with rigid shearing, and H in tetrahedral or octahedral position, are presented.

3.1 Effect of mixed mode loading on emission: the pure metal case

Quenched molecular dynamics (QMC) calculations with an EAM potential for Al-H, on a large simulation box containing a crack, are performed. The equations of motion are integrated with a Verlet algorithm, but the velocities are set to 0 when $\Sigma_i f_i \cdot v_i < 0$. The crack problem is schematically represented in Fig. 7. The simulation box is a thin parallelepiped whose sides are defined by the axes x=[111], y=[112] and z=[111]. These directions are defined in the canonical base of the fcc lattice. Periodic boundary conditions are applied in the x and y directions. The calculation is three dimensional (fcc structure), but the dimension in x is reduced. The crack is introduced along the (111) plane by "cutting the bonds" which cross the crack area defined by the crack center y_{crack} and its length 2a (of the order of $16a_0$, where a_0 is Al lattice parameter) along the y direction. The size of the box is five times larger than the crack to obtain good agreement between the stress fields calculated atomistically and the analytic solution for a crack in an infinite elastic medium, in plane strain. This geometry gives, in the x direction, an infinite crack front and an infinite dislocation line if emitted. The box size is eight times the crack length in the z direction. The particles in the three upper and lower layers, in the z direction, are fixed.

The mechanical load is applied by giving them a displacement ($U = (U_x, U_y, U_z)$). The mode I loading corresponds to a displacement in z, U_z only. Mode II is a shear obtained by U_y only and mode III by U_x. A mixed mode loading is obtained by superposition when at least two components of U are non-zero. The isotropic elastic solution is used as a starting configuration. QMD is run until the maximum force is at least lower than 10^{-3}eV/A.

The effect of mixed mode loading on dislocation emission, in the crack orientation presented above, is systematically studied in [35]. Only the $\{k_I, k_{II}\}$ space is of interest here. The crack is loaded quasi-statically. A displacement U_z is applied, the energy is minimized and, finally, the value of k_I is extracted from the T_{zz} traction profile along the crack plane by a fit to an analytical solution. Then the crack is loaded in mode II. Increasing values of U_y are applied which lead, after minimization, to k_{II} fields of increasing intensity superimposed to the k_I fields. k_{II} is extracted from the T_{yz} traction profile along the crack plane. The crack tip morphology is inspected. Dislocations are detected by their plastic displacement fields: they induce displacement discontinuities ($\Delta u_x, \Delta u_y, \Delta u_z$) across their glide plane. Δu is the difference of the displacement field just above the glide plane, and just below. In the $\{k_I, k_{II}\}$ space, two different events can occur [35]. At high values of k_I, a Shockley partial dislocation is emitted at an angle of approximately 70° from the crack plane, on the {111} plane that intersects the crack front (the crack line is the intersect). Adding k_{II} decreases the critical k_I value for emission (k_{Ie}). At moderate and low k_I values, partial Shockley dislocations are emitted in the crack plane. The case relevant to the hydrogen problem is the one where the k_I value is the maximum, without emitting a dislocation at an angle. A high k_I value will give a high triaxial stress where H atoms can segregate, in the vicinity of the crack tip. The simulations [35] show that k_I should be lower than approximately 2/3 of k_{Ie} in the absence of mode II. Once the value of k_I is fixed, a set of calculations at increasing values of k_{II} is done, until the critical value $k_{IIe}(k_I)$ is reached and the dislocation is emitted. Fig. 7b shows the variation of the Δu_y profile during such an event. An incipient dislocation appears at step 90 (see the bump in the profile at y=79). The Shockley partial is fully formed at step 100 (the displacement discontinuity approximately equals to the norm of the Burgers vector 1/6[112]=0.41) and propagates continuously into the right of the crack tip for steps higher than 100.

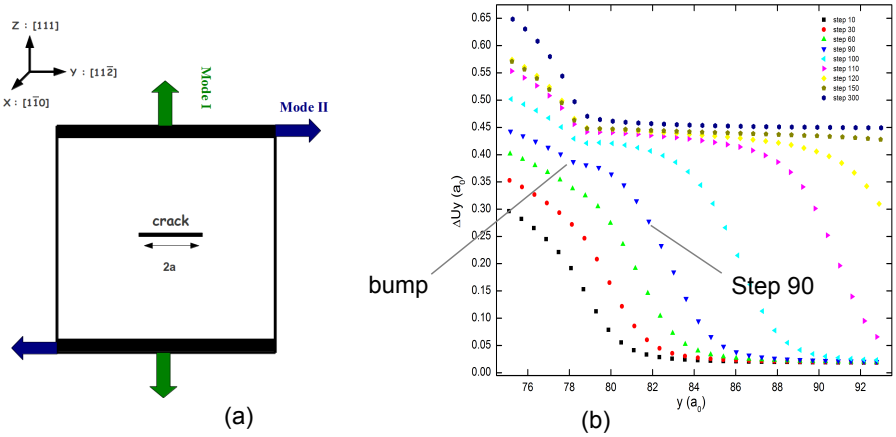

Figure 7: (a) Simulation set-up with a crack of length 2a. (b) Evolution of the displacement discontinuity in the y direction during emission and propagation of a Shockley partial in the crack plane. The crack tip is approximately at y=77a_0. The dislocation emerges at y=78a_0. a_0 is the lattice parameter of the unit cell.

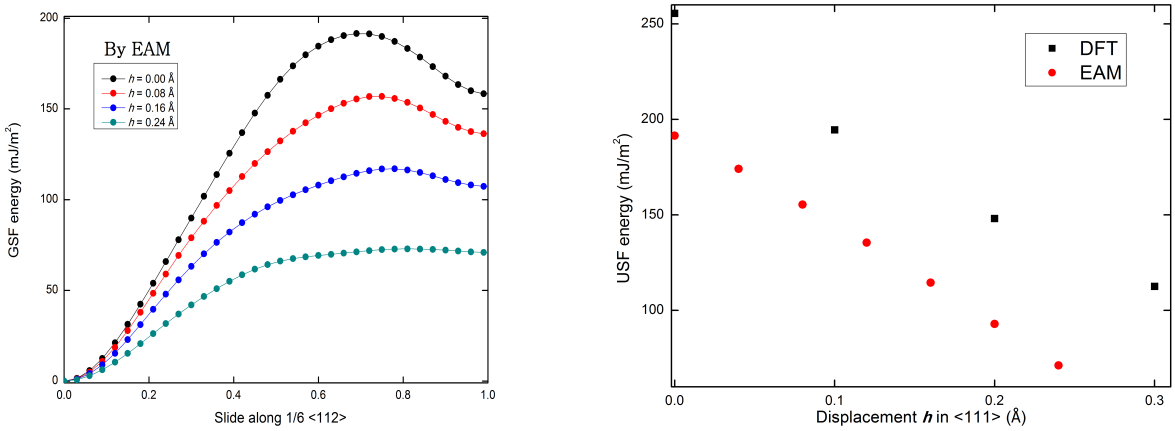

(a) (b)

Figure 8: (a) Influence of the increase of the interplanar distance on the γ surface, calculated by rigid block shearing with the EAM potential. (b) Influence of the interplanar distance on the unstable stacking energy calculated with EAM and with DFT.

Knowing where the incipient dislocation is formed, it is possible to evaluate the increase in interplanar distance δu_z at this location, as a function of k_{II}. When k_{II} is zero, δu_z is due to the mode I load only and is approximately $0.04a_0$. As k_{II} approaches k_{IIe} (k_I), the value gets close to $0.052a_0$. The influence of δu_z on the γ surface is shown on Fig. 8a. The magnitude is large: γ_{us} is reduced by almost a factor 2. Including this dependance of γ_{us} on δu_z in the Rice formula puts the theory and the atomistic calculation of k_{IIe} in excellent agreement [35]. Since γ_{us} can be calculated with small systems, it is accessible to *ab initio* methods (see Fig. 8b). Mixing crack simulations with the EAM and DFT calculations gives reliable estimates of k_{IIe}. In the next paragraph, we start extending this approach to include H atoms.

3.2 Hydrogen localization and impact on dislocation emission

An EAM potential for Al-H interactions [36] is used. It is composed of a repulsive pair part and an embedding function. It was designed to reproduce the picture drawn by the Effective Medium Theory [37]: the energy to embed a H atom in an electron gas has a minimum for electronic densities lower than the one in interstitial positions in the perfect crystal in most metals. In this density range, the embedding energy function is linear. The consequence is that a pair potential should be enough to describe Al-H in the bulk. In practice, this means that the site preference (tetrahedral is preferred to octahedral in fcc-Al) and the diffusion barrier (jump from tetrahedral to octahedral position) should be reproduced by the pair part of the potential (which includes the linear part of the embedding function and the repulsive pair interaction). The segregation to defects (where the electronic density is lower than in the bulk) should be captured by the non linear part of the embedding function (F_H). We have parametrized F_H in such a way that it has a minimum at low density and is otherwise linear. The fitting of the parameters was made on the binding energy to a vacancy, with the constraint that an off-centered position be the most favorable. The H energy at the center of the vacancy is large. Recent *ab initio* data [38] were used as guide lines and the potential [36] refitted. Its properties are now: ΔE_a=0.2eV (the activation energy for a jump from a tetrahedral position to an octahedral position), ΔE_{vac}=0.41eV (the binding energy to a vacancy in an off-center position) and ΔE_{surf}=0.46eV (binding energy to a three-fold surface site on {111}).

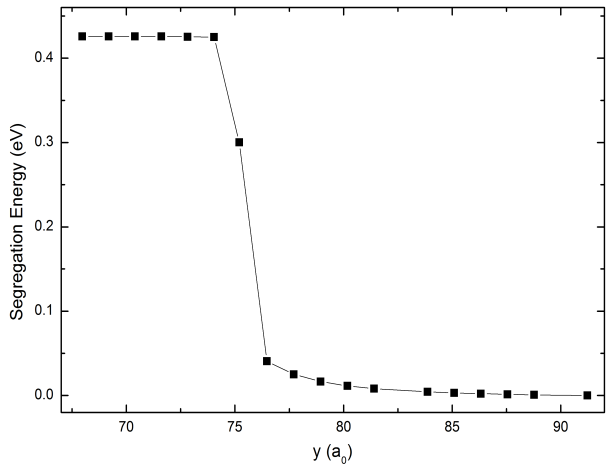

Figure 9: Hydrogen binding energy profile along the crack plane calculated by EAM.

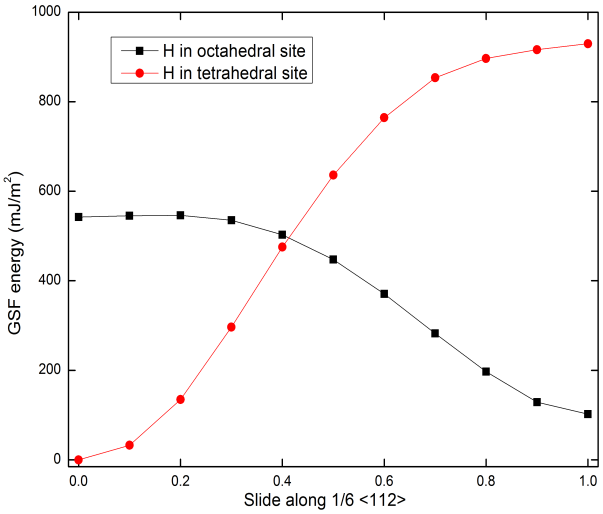

Figure 10: Generalized stacking fault energy for Al with H impurities as a function of the slip in the <112> direction, circles represent the energy for the tetrahedral site, square for the octahedral site.

This potential is used to evaluate the binding energy profile along the crack plane. On Fig. 9, the binding is the maximum on the surfaces of the crack. These energies should be increased by 0.04eV because the reference should be the unstretched crystal (long crack submitted to a low load). There is one adsorption site at the tip (ΔE_b=0.3eV). Ahead of the crack tip, the binding energy smoothly decreases as one would expect from the shape of the elastic stress field.

The influence of H on dislocation emission has been evaluated by increasing the occupation of the interstitial sites in the vicinity of the crack tip. H induced a decrease of k_{IIe} whatever the site it occupied. The maximum decrease is of the order of 20%. The relaxations are being analyzed with the goal to include them in the γ_{us} calculation.

3.3 DFT Caculations

The generalized stacking fault (GSF) energy calculations procedure in fcc-Al based on DFT theory are performed with VASP (Vienna *Ab*-initio Simulation Package) implementation [39]. The Perdew-Burke-Ernzerhof (PBE) [40] exchange-correlation functional for the generalized-gradient-approximation (GGA) is used. A plane-wave basis set is employed within the framework of the projector augmented wave (PAW) [39] method. On the basis of our tests, we have determined that a cutoff energy of 400 eV and a dense **k**-grid [41] (24x24x24 for the primitive cell), are adequate for a good convergence. The equilibrium theoretical lattice structure is determined by minimizing the Hellmann-Feynman force on the atoms and stress on the unit cell. The convergence of energy and force are set to 1.0 x 10^{-5}eV/A and 1.0 x 10^{-3}eV/A, respectively. Ground states properties of fcc-Al, H_2 and Al-H system are thus found in excellent agreement with literature [38].

We calculate the GSF energy along the <112> direction on the closed-packed (111) surface along which the glide is the easiest in fcc metals. To simulate the block shearing process we use a slab consisting of 12 atomic layers in the <111> direction. A large vacuum space of 8 atomic layers parallel to (111) plane is added between the periodically repeated slabs to avoid the interactions between two successive slabs. The top 6 atomic layers of the system are then sheared against the remaining 6 layers on the (111) plane in <112> direction. To simulate the effect of mode I at the crack tip in the GSFE calculation, a tiny displacement is imposed perpendicular to the shearing plane (i. e. along [111]).

Here we present the first results of GSFE calculations for Al with H impurities (Fig. 10). A (111) H layer is inserted in the center of Al slab at either tetra- or octa- site. Both structures are fully relaxed at first step to recover H preference at tetra-site. At shearing steps Al is relaxed only in [111] direction but H fully relaxed with no limitation. The two GSFE curves intersect at approximately half of 1/6<112>. It is qualitatively consistent with the result of Lu [33]. However the crossover corresponds to an effective γ_{us} whose value actually is nearly the double of that in our calculations of pure Al, which hints that the shearing should not occur in the plane containing the H. This point follows the findings of Apostol [34]. The author allows the reconstruction of the structure of the atoms around the H, and recover a similarly continuously increasing GSFE curve with H occupying the tetra-site in the shearing plane in addition to an expected saddle point located near to 1/6<112>. Tests have been also done with the shearing along the nearby planes, and interestingly the lowest barrier is found with the shearing occurring along the second nearest plane to the H layer.

As in the Rice model the shearing process is rigid, the full atom relaxations are not allowed. However, the EAM calculations show that the hydrogen introduction at the crack tip have important effect on the relaxation of its neighbor atoms within certain range. Hence, a local relaxation is requested for the hydrogen neighbor atoms within the same range in the GSFE calculations.

3.4 Conclusion of the dislocation emission study

In this paper, an atomistically sharp crack is studied by simulations based on EAM potentials, with loading in mixed mode to induce dislocation emission along the crack plane. It is shown in this case that the analytic formula proposed by Rice is predictive when the influence of the mixed mode loading is included in the calculation of γ_{us} (Fig. 8). The influence of H on the dislocation emission has been evaluated by introducing the increasing H occupation of the interstitial site at the crack tip. A decrease of k_{IIe} is observed with the magnitude of the decrease depending on the H localization. This points to an enhancement of plasticity at the crack tip caused by H, which is, however, opposite of the DFT findings (H increases γ_{us}). It should be noted that this estimation is undertaken with a high H concentration and the method of atomic relaxation is not verified. A more rigorous and precise DFT calculation of γ_{us} with H is required. Benefiting from the analysis of H effects at the crack tip, a reasonable approach to this calculation is proposed: the H segregation energy profile (Fig. 9) proposes in fact a quite low H concentration near the crack tip, which should be adopted similarly in the γ_{us} calculations; the analysis of the effect of H position helps indicating the most impactive interstitial site for H near the shearing plane; the range, within which H atoms have important effects on the Al atomic relaxations in the crack calculation, should be adopted for the local relaxation in the γ_{us} calculation. The agreement between the theory (γ_{us}) and the calculation of k_{IIe} under the effect of H is expected to confirm that H could enhance the dislocation emission at the crack tip.

4. CONCLUSION

Nous avons abordé, par simulation atomistique, deux mécanismes en compétition à la pointe d'une fissure fine intergranulaire: l'endommagement par des cavités nanométriques et l'émission de dislocations par la pointe elle même, en présence ou non d'hydrogène. Les chargements critiques obtenus (tableau 1) montrent que même dans la configuration de plus forte densité de cavités, l'émission de dislocations est toujours plus facile que la rupture. On estime que $k_I^c \sim 1.2 k_I^e$ (à partir du tableau 1 en considérant que la rupture a lieu, en gros, pour un chargement de 5 et l'émission pour un chargement de 4, en unités de déplacement au bord de la boîte). En regardant les valeurs d'énergie de faute instable (γ_{us}), obtenues en EAM et en DFT (Fig. 8b), on voit que le modèle EAM utilisé dans les calculs de rupture sous-estime γ_{us} de 20%. On a donc $k_I^{e\ DFT} \sim 1.1 k_I^{e\ EAM}$, ce qui pourrait réduire l'écart entre k_I^c et k_I^e. Une des raisons qui pourrait expliquer que la fissure ne se comporte pas de manière fragile, même avec une densité initiale importante de cavités (Fig. 6b), peut être la durée trop courte des simulations. Des temps physiques de l'ordre de quelques pico secondes ne permettent pas de voir les cavités croître à un niveau de contrainte suffisamment faible pour donner $k_I^c < k_I^e$. Nous nous orientons vers l'étude des mécanismes de croissance de cavités, aux "grandes" échelles de temps. Il est crucial de comprendre dans quel sens H modifie k_I^e. Les calculs ab initio recents ne sont malheureusement pas d'une grande aide parce qu'ils sont contradictoires. Ils prédisent: une forte diminution [33], une forte augmentation [42], les deux (selon les reconstructions) [34]... Les calculs EAM que nous avons effectués en pointe de fissure montrent essentiellement que l'effet sera faible (négligeable par rapport à l'effet de chargement en mode mixte), en partie parce que H peut diffuser en même temps que l'émission de la dislocation mais aussi parce que les concentrations locales sont faibles en sous-surface. Cette conclusion n'est pas valable dans les systèmes où les hydrures peuvent être stabilisés, en particulier par un effet de contrainte locale [25,26].

5. REMERCIEMENTS

Ce travail est supporté par le programme ANR EcHyDNA (Blanc10_19424). Les auteurs remercient le centre de calcul HPC de CALMIP (CICT Toulouse) pour les resources 2011 et 2012-p0749.

6. RÉFÉRENCES

[1] H. K. Birnbaum, I. M. Robertson, P. Sofronis and D. Teter, 1997, "Mechanisms of Hydrogen Related Fracture-A review", proceedings of CDI'96, Th. Magnin ed., The Institute of Materials
[2] G.M. Scamans, R. Alani, P. R. Swann, 1976, "Pre-exposure embrittlement and stress corrosion failure in AlZnMg alloys", Corr. Sci. **16** p. 443.
[3] M.L. Martin et al., 2012, "Hydrogen-induced intergranular failure in nickel revisited", acta mater. **60** pp. 2739-2745
[4] I.-H. Lin and R. Thomson, 1986, "Cleavage, dislocation emission, and shielding for cracks under general loading" acta metall. 34 pp.187-206
[5] J. R. Rice and R. Thomson, 1974, "Ductile versus brittle behavior of crystals", Phil. Mag. **29** pp. 73-97
[6] S. J. Zhou, A. E. Carlsson and Robb Thomson, 1994, "Crack blunting effects on dislocation emission from cracks", Phys. Rev. Lett. **72** pp. 852-855
[7] S. J. Zhou, A. E. Carlsson and Robb Thomson, 1993, "Dislocation nucleation and crack stability: Lattice Green's-function treatment of cracks in a model hexagonal lattice", Phys. Rev. B **47** pp. 7710-7719
[8] R. P. Gangloff, 2003, "Hydrogen assisted cracking of high strength alloys", in: I. Milne, R.O. Richie, B. Karihaloo (Eds.), Comprehensive structural intergrity, volume **6**, Elsevier Science New York, NY, p. 31.
[9] D. E. Jiang and E. A. Carter, 2004, "First principles assessment of ideal fracture energies of materials with mobile impurities: implications for hydrogen embrittlement of metals", acta mater. 52 pp. 4801-4807
[10] A. Van der Ven and G. Ceder, 2004, 'The thermodynamics of decohesion", acta mater. **52** pp. 1223-1235

[11] D. Tanguy and T. Magnin, 2003, "Atomic-scale simulation of intergranular segregation of H in Al-Mg: implications for H-induced damage", Phil. Mag. **83** pp. 3995-4009
[12] C. J. McMahon, 1999, "Overview: time-dependent interfacial decohesion", Mater. Sci. Eng. A **260** vii-x
[13] S. Serebrinsky, E. A. Carter and M. Ortiz, 2004, "A quantum-mechanically informed continuum model of hydrogen embrittlement", JMPS **52** pp. 2403-2430
[14] M. Shiga, M. Yamaguchi and H. Kaburaki, 2003, "Structure of clean and hydrogenated Ni surfaces and symmetrical tilt grain boundaries using the embedded-atom method", Phys. Rev. B **68** art. 245402
[15] M. Dadfarnia et al., 2008, "Modeling issues on hydrogen-induced intergranular cracking under sustained load", Proceedings of the 2008 International Hydrogen Conference B. somerday, P. Sofronis and R. Jones Ed. pp.613-621
[16] D. Tanguy, 2011, "Monte Carlo Methodology for Grand Canonical Simulations of Vacancies at Crystalline Defects", Applications of Monte Carlo Method in Science and Engineering, Shaul Mordechai (Ed.), ISBN: 978-953-307-691-1, InTech, Available from: http://www.intechopen.com/articles/show/title/monte-carlo-methodology-for-grand-canonical-simulations-of-vacancies-at-crystalline-defects
[17] D. Tanguy and M. Mareschal, 2005, "Superabondant vacancies in a Metal-Hydrogen system : Monte Carlo simulations.", Phys. Rev. B **75** art 174116
[18] E. Vamvakopoulos and D. Tanguy, 2009, "Equilibrium vacancy concentrations in Al-Σ=33(554)[110] by Grand Canonical Monte Carlo Simulations", Phys. Rev. B **79** art. 094116
[19] V. Yamakov, E. Saether, D.R. Phillips, and E.H. Glaessgen, 2005, "Dynamic Instability in Intergranular Fracture", PRL **95** art. 015502
[20] D. Tanguy, 2007, "Constrained molecular dynamics for quantifying intrinsic ductility versus brittleness", Phys. Rev. B **76** art. 144115
[21] P. Sofronis, 1995, "The influence of Mobility of Dissolved Hydrogen on the Elastic Response of a Metal", J. Mech. Phys. Solids 43 pp. 1385-1407.
[22] J. P. Chateau, D. Delafosse and Th. Magnin, 2002, "Numerical simulations of hydrogen–dislocation interactions in fcc stainless steels.: part I: hydrogen–dislocation interactions in bulk crystals", Acta. Mater 50 pp. 1507-1522.
[23] M. S. Daw and M. I. Baskes, 1984, "Embedded-Atom Method - Derivation and Application to impurities, surfaces, and other defects in metals", Phys. Rev. B 29 pp. 6443-6453.
[24] J. E. Angelo, N. R. Moody and M. I. Baskes, 1995, "Trapping of Hydrogen to Lattice-defects in Nickel", Mod. Sim. Mat. Sci. Eng. 3 pp. 289-307.
[25] J. von Pezold, L. Lymperakis and J. Neugebeauer, 2011, "Hydrogen-enhanced local plasticity at dilute bulk H concentrations: The role of H–H interactions and the formation of local hydrides", Acta Mater. 59 pp. 2969-2980.
[26] J. Song and W. A. Curtin, 2011, "A nanoscale mechanism of hydrogen embrittlement in metals", Acta Mater. 59 pp. 1557-1569.
[27] J. R. Rice and R. Thomson, 1974, "Ductile versus brittle behavior of crystals", Phil. Mag. 29 pp. 73-97.
[28] J. R. Rice, 1992, "Dislocation nucleation from a crack tip - an analysis based on the Peierls concept", J. Mech. Phys. Solids 40 pp. 239-27.
[29] V. Vitek, 1968, "Intrinsic stacking faults in body-centered cubic crystals", Phil. Mag. 18 p. 773
[30] S. J. Zhou, A. E. Carlsson and Robb Thomson, 1994, "Crack blunting effects on dislocation emission from cracks", Phys. Rev. Lett. 72 pp. 852-855.
[31] Y. M. Juan, Y. Sun and E. Kaxiras, 1996, "Ledge effects on dislocation emission from a crack tip: A first-principles study for silicon", Phil. Mag. Lett. 73 p.233.
[32] S. J. Zhou, A. E. Carlsson and Robb Thomson, 1993, "Dislocation nucleation and crack stability: Lattice Green's-function treatment of cracks in a model hexagonal lattice", Phys. Rev. B 47 pp. 7710-7719.
[33] G. Lu et al., 2002, "Energetics of hydrogen impurities in aluminum and their effect on mechanical properties", Phys. Rev. B 65 p. 064102.
[34] F. Apostol and Y. Mishin, 2011, "Hydrogen effect on shearing and cleavage of Al: A first-principles study", Phys. Rev. B 84 p. 104103.
[35] K. Gouriet and D. Tanguy, 2012, "Dislocation emission from a crack under mixed mode loading studied by molecular statics", Phil. Mag. **92** pp. 1663-1679.
[36] D. Tanguy and T. Magnin, 2003, "Atomic-scale simulation of intergranular segregation of H in Al-Mg: implications for H-induced damage", Phil. Mag. 83 pp. 3995-4009.
[37] J. K. Norskov and F. Besenbacher, 1987, "Theory of hydrogen interaction with metals", Journal of Less-Common Metals 130 pp. 475-490.
[38] C. Wolverton, V. Ozolins and M. Asta 2004, "Hydrogen in aluminum: First-principles calculations of structure and thermodynamics", Phys. Rev. B 49, 144109.
[39] G. Kresse and J. Hafner, Phys. Rev. B 48 (1993) 3115, G. Kresse and J. Furthmüller, Comput. Mater. Sci. 6 (1996) 15, Phys. Rev. B **54** (1996) 11169, G. Kresse and D. Joubert, Phys. Rev. B 59 (1999) 1758.
[40] J.P. Perdew, K. Burke, M. Ernzerhof, Phys. Rev. Lett. 77 (1996) 3865, ibid. **78** (1996) 1396.
[41] H.J. Monkhorst and J.D. Pack 1978, "Special points for Brillouin-zone integrations", Phys. Rev. B 13 (1976) 5188.
[42] R.J. Zamora et al. 2012, "*Ab initio* prediction of environmental embrittlement at a crack tip in aluminium", Phys. Rev. B **86** 060101.